JOURNAL OF MATERIALS SCIENCE **40** (2005) 5603–5608

Advances in DLC coatings by hybrid PSII and PECVD as a barrier to corrosion in simulated body fluid*

CHENGLONG LIU*
Department of Materials Engineering, Dalian University of Technology, Dalian, 116024, P. R. China; State Key Laboratory for Material Modification by Laser, Ion and Electron Beams, Dalian University of Technology, Dalian, 116024, P. R. China
E-mail: liucl@student.dlut.edu.cn

DAZHI YANG, MIN QI
Department of Materials Engineering, Dalian University of Technology, Dalian, 116024, P. R. China

XINLU DENG
State Key Laboratory for Material Modification by Laser, Ion and Electron Beams, Dalian University of Technology, Dalian, 116024, P. R. China

Published online: 25 August 2005

In this study, diamond-like carbon (DLC) films were deposited on biomedical AISI316L stainless steel by hybrid plasma source ion implantation (PSII) and plasma-enhanced chemical vapour deposition (PECVD). Potentiodynamic polarization tests and Electrochemical Impedance Spectroscopy (EIS) have been employed to investigate the corrosion performance of different DLC films in Tyrode's simulated body fluid (pH = 7.4). The corrosion resistance of the DLC films by PECVD deteriorated rapidly after 24 h of immersion, but those made by hybrid PSII and PECVD offered more effective barrier for AISI316L stainless steel during 72 h of immersion. The test results demonstrated that the DLC film by hybrid PSII and PECVD possessed less corrosion current density, greater corrosion resistance, and more positive breakdown potential in simulated body fluid.

1. Introduction

AISI316L stainless steel has been widely used for biomedical implants, such as orthopedic, cardiovascular applications and dental devices. As implants, they are exposed to body fluid and cells, a corrosive circumstance. Corrosion of the implant can lead to cellular damage, infections, blood coagulation (potentially leading to thrombosis) and failure of the implants [1].

Coating biomedical implants with protective films may extend the lifetime of implants for the benefit of the patients. Diamond-like carbon films have shown great potential as protective coatings for improving the performance of biomedical devices [2]. However, problems exist including poor adhesion to some metallic substrates [3] and limited corrosion resistance due to the existence of microscopic pinholes in the DLC films by PVD or CVD [4], which causes the breakdown of DLC films in liquid environments.

Plasma source ion implantation (PSII) has been used to enhance the adhesion strength of DLC films on different substrates [6]. The results of corrosion tests showed that the DLC films by PSII improved the corrosion performance of Ni and C1018 steel in the solution including borate and chloride to a limited extent [7, 8]. Chen [9] pointed out that the wear and corrosion properties for 304 stainless steel and Ti6Al4V alloy modified by carbon implantation was dependent on implantation layer composites and structure. In this study, two kinds of DLC films were deposited on biomedical AISI316L stainless steel by different methods, respectively. The influence of DLC coatings on the corrosion behavior of AISI316L stainless steel was evaluated in Tyrode's simulated body fluid, and consideration was also given to the mechanical properties and the microstructure.

2. Experimental details

A twinned microwave ECR (875G, 2.45 GHz) plasma source with a cusp magnetic field was used to generate

*Author to whom all correspondence should be addressed.
0022-2461
DOI: 10.1007/s10853-005-1426-9

a high-density plasma [10]. Biomedical AISI316L stainless steel samples measuring 12 mm in diameter and 2 mm in thickness were utilized as the substrates. The substrates were ground and polished to obtain a mirror-like surface, and then cleaned using an ultrasonic cleaner in acetone followed by an alcohol rinse. Prior to deposition, samples were etched with an argon plasma for 15 min to eliminate the native oxide on their surfaces. Methane of purity 99.9% was used as carbon source. The base pressure was pumped below 3×10^{-3} Pa before deposition. Two methods were applied to generate DLC films: (a) PECVD was used. The films were deposited using a gas mixture of argon and methane at a RF negative bias of 300 V; (b) Both preliminary PSII of the substrate and subsequent PECVD were applied. Firstly, under a high negative bias 20 KV (10 μs/250 Hz) a carbon implanted layer was prepared from methane. The deposition time was 60 min. Then by use of PECVD DLC films were achieved. The substrates were water-cooled during deposition. The film was about 1 μm in thickness by controlling the deposition time. The following notation is applied to identify both kinds of the samples: DLC_{PECVD}/AISI316L and $DLC_{PSII+PECVD}$/AISI316L.

Raman spectroscopy was used to characterize the structure of the films. A 514.5-nm Ar laser at a power of 2 mW was used as the excitation source. All Raman data acquisitions were obtained at room temperature.

The measurement of adhesion strength was performed on a (CSR-01) scratch tester equipped with a 120° diamond indenter by sliding along the surface of the film with the loading speed of 2000 gf min^{-1}.

Samples of DLC/AISI316L were studied in Tyrode's simulated body fluid (TSBF, pH = 7.4) at the temperature of 37 ± 1°C. A sheet of copper was attached onto the uncoated side of the specimen, which was cold-mounted by olefin with a 1 cm^2 monitoring area of the coatings. The experimental set-up consisted of a conventional three-electrode cell containing the working electrode, a saturated calomel electrode (SCE) and a platinum sheet as the counter electrode.

Potentiodynamic polarization was utilized to monitor the polarization curves of all the samples by an EG&G Potentiostat/Galvanastat model 273 at a scan rate of 1 mV/s. The initial scan potential was 200 mV below corrosion potential (E_{corr}). All measurements were normally conducted after 30 min of immersion.

Electrochemical Impedance Spectroscopy (EIS) measurements were carried out by an EG&G Potentiostat/Galvanastat model 283 after different immersion periods. The frequency range was $3 \times 10^4 - 10^{-3}$ Hz. Fifty points were measured at an amplitude of 15 mV. For convenience the analysis of the spectra was performed with ZSimpWin software.

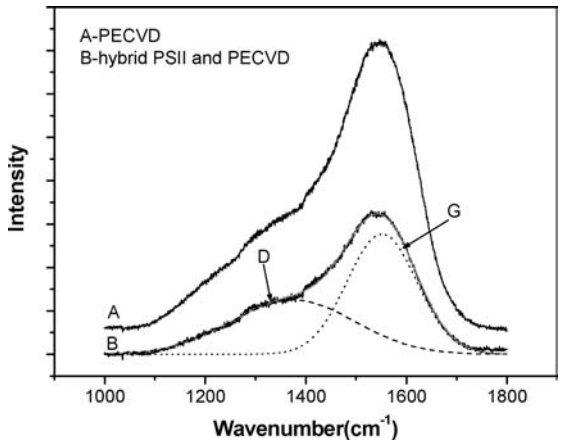

Figure 1 Raman spectra of the films prepared by PECVD and hybrid PSII and PECVD methods.

3. Results and discussions

3.1. Raman spectroscopy

The Raman spectra of films deposited on AISI316L are shown in Fig. 1. Both spectra present two peaks that can be fitted by two Gaussian curves. The peak at about 1350 cm^{-1} can be ascribed to the D peak (due to aromatic ring deformation in disordered graphite phases). The peak at approximately 1550 cm^{-1} can be identified with the *G* peak (ascribed to the localized sp^2 carbon C=C bonds in crystalline graphite) [11]. Table I shows the Raman parameters determined respectively from both Raman spectra, which demonstrates that both films are characteristic of conventional hydrogenated amorphous carbon (α-C:H) [12].

Table I shows the I_D/I_G intensity ratio value for the $DLC_{PSII+PECVD}$ films is larger than that for the DLC_{PECVD} film, and moreover the *G* peak maximum intensity position shifts to higher wave number, which indicates that the disorder degree in the DLC_{PECVD} films is bigger than in the $DLC_{PSII+PECVD}$ films. For the DLC_{PECVD} films, compared with the $DLC_{PSII+PECVD}$ film, the fraction of six carbon atom rings in the crystalline graphite phase decreases or the fraction of linear chain groups constituted mainly by sp^3 carbon bonded increases [13]. According to Qian *et al*. [14], the value of $I_D/I_G = 0.8$ is characteristic of α-C:H films containing 50–60% of diamond-like carbon. As I_D/I_G ratio values are approximately 0.806 and 0.945 respectively in Fig. 1, it can be suggested that there exist more

TABLE I Raman parameters for the DLC_{PECVD} and $DLC_{PSII+PECVD}$ films Raman spectra

		D peak		G peak	
Type of films	I_D/I_G	Position (cm^{-1})	Half-width (cm^{-1})	Position (cm^{-1})	Half-width (cm^{-1})
DLC_{PECVD}	0.806	1385.6 ± 0.9	245.1 ± 0.4	1551.6 ± 0.3	138.1 ± 0.7
$DLC_{PSII+PECVD}$	0.945	1375.6 ± 0.4	255.6 ± 0.4	1553.8 ± 0.2	129.3 ± 0.6

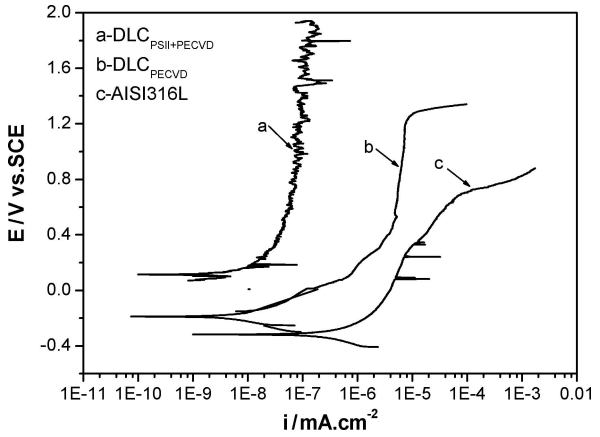

Figure 2 Polarization curves of the uncoated and DLC films coated AISI316L in Tyrode's simulated body fluid: (a) $DLC_{PSII+PECVD}$/AISI316L; (b) DLC_{PECVD}/AISI316L; (c) AISI316L without coatings.

than 60% diamond-like carbon in the two films coating AISI316L.

3.2. Potentiodynamic polarization tests

In this study, the measurements were carried out in TBSF. The polarization curves for AISI316L with and without DLC coatings in three groups are shown in Fig. 2. Although the complete DLC film is an isolating barrier layer and is supposed to cover the whole substrate surface, some substrate sites are still exposed to the electrolyte due to the depositing methods, where micropores exist in the protective films [14]. Obvious changes in the corrosion potential, E_{corr}, have occurred for AISI316L coated by DLC films, which are more positive than that of the substrate. The E_{corr} of the $DLC_{PSII+PECVD}$/AISI316L samples is less negative than that of the DLC_{PECVD}/AISI316L samples. It can be suggested that the $DLC_{PSII+PECVD}$ coating should be more compact than the DLC_{PECVD} coating through the difference of E_{corr}. During potentiodynamic polarization, the $DLC_{PSII+PECVD}$ films were not destroyed completely, while existing localized breakdown and rapid repair; but for the DLC_{PECVD} film, the samples failed at the potential of about 1300 mV. The corrosion current density measured based on the cathodic part of the polarization curve is an important parameter to evaluate the kinetic of corrosion reactions, to which the corrosion rate is normally proportional. One can observe how the bare substrate corroded more quickly than the coated AISI316L samples. For the DLC_{PECVD} coated samples, the corrosion rate decreases to approximately 1/20 that of the substrate. For the $DLC_{PSII+PECVD}$ coated samples, the corrosion current is two orders of magnitude smaller than that of AISI316L without coatings. These data indicate that the $DLC_{PSII+PECVD}$ films offer more effective protection for AISI316L in Tyrode's simulated body fluid.

3.3. Electrochemical impedance spectroscopy (EIS) tests

In this study, EIS has been applied to detect micropores in DLC films and their effect on the corrosion-resistance behavior over long immersion time has been assessed. In the Bode plot, impedance at high frequency represents the response of the coating, thus exhibiting the coating information, while at the low frequency limit, the information about process is related to the reaction on the substrate/solution interface.

Fig. 3 gives the Bode plots from the DLC_{PECVD} coated samples over different immersion times in TBSF. According to the impedance diagram, after 1 h of immersion, only one semi-circle was shown, corresponding to one-time constant from the samples. In fact, such a short period of immersion time is too short to reveal any degradation of the substrate. When the immersion period is greater than 48 h, the phase shift is different to that of 1 h. In the low frequency range, approximately 10^1–10^{-2} Hz, the impedance is dominated by a capacitance, and the phase shift is close to -70°, which indicates that the solution has penetrated into the coating/substrate interface via micropores and the second time constant related to the solution/substrate has been resolved. In the high frequency range, approximately 10^4–10^5 Hz, an ohmic behavior is shown and the phase shift tends to -6°. In the medium frequency range, approximately 10^1–10^4 Hz, the phase shift after 2 h of immersion starts increasing and then decreases, compared to the monotonic increase of that after 1 h of immersion, which is an indication of the

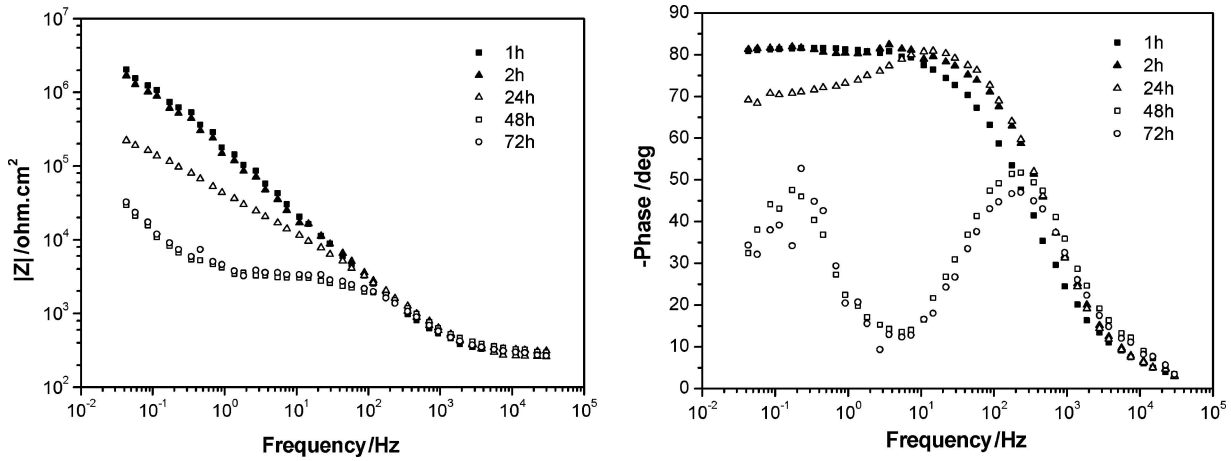

Figure 3 Bode plots of the DLC_{PECVD}/AISI316L samples in Tyrode's simulated body fluid measured over the different immersion periods.

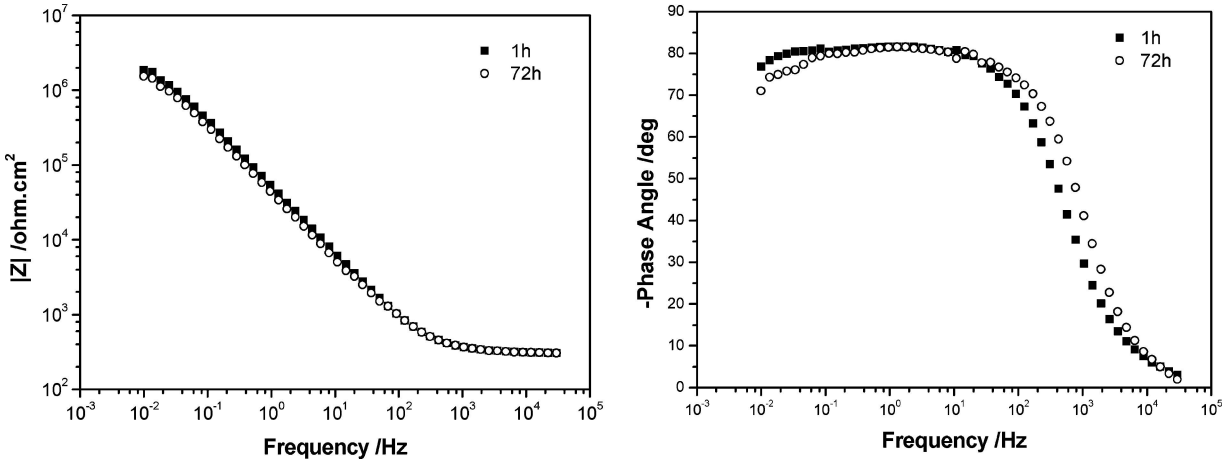

Figure 4 Bode plots of the DLC/AISI316L samples by hybrid PSII and PECVD in Tyrode's simulated body fluid measured over the immersion period of 1 h and 72 h.

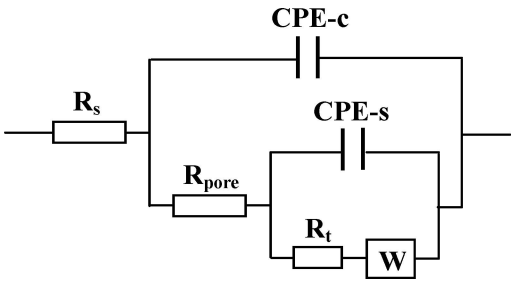

Figure 5 Equivalent circuit used for DLC_{PECVD}/AISI316L.

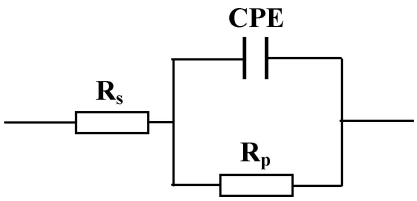

Figure 6 Equivalent circuit for $DLC_{PSII+PECVD}$/AISI316L where R_p is the polarization resistance and CPE is the constant phase element of the coating.

occurrence of the double layer capacitance between the substrate and the solution. Thereby, the galvanic corrosion cells were established, and the localized corrosion dominated the corrosion processes [15]. In such a case, the electrochemical interface can be subdivided into two sub-interfaces [16]: TSBF/DLC_{PECVD} and TSBF/substrate. This type of EIS spectra of the DLC_{PECVD}/ AISI316L samples in the solution including Cl^- is best modeled by an equivalent circuit (EC) proposed by Pakonslantinou *et al.* [17] and Liu *et al.* [15] for the two sub-electrochemical interfaces, shown in Fig. 5. The equivalent circuit consists of the following elements: the solution resistance of the test TSBF R_s; the dielectric property of the coating presented by a pair of elements CPE-*c* (*c* means coating) and R_{pore}; the double-layer capacitance and polarization charge transfer resistance at DLC_{PECVD}/AISI316L interface at micropores CPE-*s* (*s* means substrate) and R_t.

Constant phase element (CPE) is usually used instead of a capacitance to account for the non-ideal capacitance response due to almost no existence of pure capacitance in the real electrochemical process:

$$Z_{(CPE)} = {}^{1}/_{[Yo\,(j\varpi)]}^{\eta} \qquad (1)$$

where Y_O is a constant and ϖ is the angular frequency, η is a mathematic expression ($0 \leq \eta \leq 1$) [15]. For $\eta = 0$ it stands for resistance, while it is capacitance of $\eta = 1$. And $0 < \eta < 1$ represents the deviation of ideal capacitance, which is related to the surface roughness [17].

The Bode plots for the $DLC_{PSII+PECVD}$/ AISI316L sample taken after 1 h and 72 h of immersion are presented in Fig. 4, respectively. As seen in the figure the data at 72 h differ little from that at 1 h, and can be interpreted by the following equivalent circuit (Fig. 6), including a double-layer capacitance in parallel with the polarization resistance, besides the solution resistance. Over the whole immersion time, the impedance decreases with immersion time increasing, which indicates little weakening of the $DLC_{PSII+PECVD}$ film when solution slowly penetrated into the coating through the micropores, and the phase shift at 1 h is similar to that at 72 h. This model takes into account that the $DLC_{PSII+PECVD}$ films are less porous than the DLC_{PECVD} films.

Table II summarizes the circuit parameters using the fitting circuits in Figs 5 and 6. Fitting errors are less than 10% for both samples. For the DLC_{PECVD}/ AISI316L samples, following further immersion, Q_c increased indicating the exposed coating area increased due to uncovering of porosity [19]. However, the higher η-Q_c value of 0.94 at the immersion time of 1 h indicates a strong capacitive response between TSBF and the film at the initial exposure time and no degradation of the substrate was revealed. The decreases of η-Q_c value and R_{pore} as immersion time increases imply that with the increased number of opening micropores the protective performance of DLC_{PECVD} coatings was weakened and became more conductive. Obviously the exposed area will increase as immersion time extends. Because the opening micropores exist in the DLC_{PECVD} coating, Warburg (*W*) impedance is readily an appropriate diffusion element to describe this as a semi-infinite

TABLE II Electrochemical parameters obtained from EIS spectra using the equivalent circuit in Figs 5 and 6 for the DLC_{PECVD}/AISI316L and $DLC_{PSII+PECVD}$/AISI316L samples in Tyrode's simulated body fluid

Samples DLC_{PECVD}/AISI316L	$R_s/\Omega\ cm^2$	$Q_c/\mu F\ m^{-2}$	η- Q_c	$R_{pore}/\Omega\ cm^2$	$Q_s/\mu F\ cm^{-2}$	η- Q_s	$R_t/\Omega\ cm^2$	$W/\mu/cm^2\Omega\sqrt{s}$
1 h	29.78	1.57×10^{-1}	0.94	7.31×10^6	–	–	–	–
2 h	36.52	1.63×10^{-1}	0.89	7.28×10^6	3.37	0.98	9.27×10^6	755
24 h	26.47	7.75	0.81	6.76×10^5	9.91	0.85	6.07×10^6	1238
48 h	25.04	10.23	0.79	6.19×10^4	28.16	0.67	3.89×10^6	7645
72 h	32.65	21.56	0.73	5.84×10^4	79.12	0.74	8.7×10^6	9981
$DLC_{PSII+PECVD}$/AISI316L		$R_s/\Omega\ cm^2$		$Q_c/\mu F\ cm^{-2}$		η- Q_c		$R_p/\Omega\ cm^2$
1 h		25.27		1.67×10^{-1}		0.934		1.93×10^7
72 h		30.21		1.49×10^{-1}		0.927		2.01×10^7

length diffusion, which is a parameter containing diffusion coefficient and characteristic of stagnant layer. With the increase of immersion time, the more formation of occluded cells caused the increase of oxygen near the coating. Moreover the improvement of conductive property for the DLC_{PECVD} coatings caused the decrease of R_t. The above two factors contribute to the increase of W with immersion period.

The results of potentiodynamic polarization and EIS tests indicate that compared to the DLC_{PECVD} coatings, the $DLC_{PSII+PECVD}$ coatings have less porosity and higher corrosion resistance, and can offer better barrier for biomedical AISI316L in TSBF. The lower E_{corr} of DLC_{PECVD}/AISI316L samples after the immersion of 1 h, when compared to the $DLC_{PSII+PECVD}$/AISI316L samples, indicates the thermodynamic stability decreased more quickly as the solution reached the substrate through the micropores in the films. The existing intergranular defects and adhesion strength for two kinds of samples may differ due to the different preparation techniques, thus yielding different corrosion performance. Morshed [20] pointed out that the adhesion of DLC films directly on AISI316L depended on the length of etching time with an argon atom beam, which could cause the change of oxides on its surface. It can be suggested that the adhesion strength be determined by the type of oxides on the surface for the DLC_{PECVD} film. Moreover, because of the inevitable shortcomings of the CVD techniques there are almost always micropores even in good quality CVD DLC films [21]. For DLC films by hybrid PSII and PECVD, carbon implantation by PSII can result in its enhanced adhesion to the substrate. An improvement in adhesion strength occurs due to ion mixing at the coating/substrate interlayer and between the film layers [22]. A graded interface, consisting of carbides can be produced by the carbon implantation process [6], which improves the match between film and film or film and substrate, causing the release of residual stress. The adhesion strength of $DLC_{PSII+PECVD}$ films on the substrate is about 1.5 times of magnitude larger than that of DLC_{PECVD} films, which is about 47.7 N. The improvement of adhesion strength can effectively suppress the penetration of the solution and the destruction of DLC films under the action of aggressive solutions [23]. On the other hand, the higher value of R_P observed in the $DLC_{PSII+PECVD}$ films shows that the micropores in the film are not completely open, which also decreases the possibility of the solution penetrating into the DLC/AISI316L interlayer through the micropores and attacking the substrate surface, leading to its dissolution and subsequent oxide precipitation inside the micropores [4]. Therefore, the thermodynamic stability of $DLC_{PSII+PECVD}$/AISI316L samples is superior to that of DLC_{PECVD}/AISI316Lsamples. Once the solution reaches the substrate through the micropores in the films, the substrate could be broken by the localized corrosion. For the $DLC_{PSII+PECVD}$/AISI316L samples, the micropores expose the carbon implanted layer, C-C bonded carbon or a combination of both [8], and owing to the formation of metastable layers carbon implantation is effective for corrosion protection [24]. For the DLC_{PECVD}/AISI316L sample, due to the absence of metastable layers, these micropores act as initial sites for breakdown and the galvanic corrosion is established. To maintain charge neutrality, Cl^- must migrate into the micropores, causing the chloride concentration to increase. The formation of a critical propagation solution is considered to be the second step in the breakdown process. After removal from TBSF the DLC_{PECVD}/AISI316L samples were covered with copious pitting holes with corrosion products. Moreover the DLC_{PECVD} film flaked away from the substrate.

According to the EIS data, one can observe, the breakdown of DLC_{PECVD}/AISI316L occurred at only 24 h. In comparison, few changes were shown for $DLC_{PSII+PECVD}$/AISI316L after 72 h of immersion. Therefore, it is necessary to prolong the test time to measure its real lifetime in TBSF for biomedical applications.

4. Conclusions

We have used the hybrid PSII and PECVD to deposit DLC coatings and investigated their effects on mitigating the breakdown of AISI316L stainless steel in TSBF (pH = 7.4). The disorder degree in the DLC_{PECVD} films was greater than that in the $DLC_{PSII+PECVD}$ films. Both coatings showed improvement in suppressing the susceptibility to pitting corrosion, while $DLC_{PSII+PECVD}$ films provided more effective barrier against pitting corrosion, and no breakdown potential was observed. The EIS results showed similar tendency to the one observed in potentiodynamic polarization tests. The initial impedance of AISI316L coated with the $DLC_{PSII+PECVD}$ film was bigger than that of the DLC_{PECVD} sample, which reflects the

structural differences of both coatings. Compared to the $DLC_{PSII+PECVD}$/AISI316L samples, the breakdown time of the DLC_{PECVD}/AISI316L samples was too short for biomedical applications, and the films flaked away from the substrate after 72 h of immersion. For the $DLC_{PSII+PECVD}$ films, there is a minimum time required for total penetration of solution into the film/substrate interlayer.

Acknowledgments

The project is supported by the national natural science fund of China under the contract No. 50081001 and NAMCC 863 (No. 2002AA326010). The authors express their gratitude to Prof. Liang C.H., Prof. Peng Q. and Dr Chen W. for supporting the EIS tests (School of Chemical Engineering, DUT China).

References

1. A. GRILL, *Diam. Rel. Mater.* **12** (2003) 166.
2. R. HAUERT and U. MULLER, *ibid.* **12** (2003) 171.
3. C. DUMKUM, D. M. GRANT and I. R. MCCOLL, *ibid.* **6** (1997) 802.
4. A. ZENG, E. LIU, I. F. ANNERGREN, *et al., ibid.* **11** (2002) 160.
5. M. A. S. OLIVEIRA, A. K. VIEIRA and M. MASSI, *ibid.* **12** (2003) 2136.
6. K. C. WALTER, M. NASTAS and C. MUNSON, *Surf. Coat. Technol.* **93** (1997) 287.
7. R. S. LILLARD, D. P. BUTT and T. N. TAYLOR, *Corr. Sci.* **39**(9) (1997) 605.
8. R. S. LILLARD, D. P. BUTT, N. P. BAKER, *et al., Sur. Eng.* **15**(3) (1999) 221.
9. J. CHEN, J. R. CONRAD and R. A. DODD, *J. Mater. Proc. Technol.* **49** (1995) 115.
10. TANG LI XIN, ZHEN-AN DENG XIN-LU *et al., J. Wuhan Uni. Technol.-Mater. Sci. Ed. Cont.* **19**(2) (2004) 44.
11. CHU HSIAO, TSAI and D. B. BOGY, *J. Vac. Sci. Technol. A* **5**(6) (1987) 3287.
12. K. BABA and R. HALADA, *Surf. Coat. Technol.* **235** (1998) 103.
13. G. T. BURSTEIN and R. M. SOUTO, *Electrochim. Acta* **40**(12) (1995) 1881.
14. F. QIAN, P. K. SINGH, S. K. DUTLA, *et al., Appl. Phys. Lett.* **67** (1995) 3120.
15. C. LIU, Q. BI and A. MATTHEWS *Corr. Sci.* **43** (2001) 1953.
16. C. LIU, A. LEYLAND, S. LYON, *et al., Surf. Coat. Technol.* **76–77** (1995) 615.
17. P. PAPAKONSTANTINOU, J. F. ZHAO and P. LEMOINE, ET AL., *Diam. Rel. Mater.* **11** (2002) 1074.
18. A. NORLIN, J. PAN and C. LEYGRAF, *Biomol. Eng.* **19** (2002) 67.
19. B. ELSENER, A. ROTA and H. BOHIN, *Mater. Sci. Forum* **44/45** (1989) 29.
20. M. M. MORSHED, B. P. MCNAMARA, D. C. CAMERON, ET AL., *Surf. Coat. Technol.* **163–164** (2003) 541.
21. V. NOVOTNY, K. H. LAI, C. Y. CHAN, *et al., J. Elechtrochem. Soc. Electrochem. Sci. Technol.* **135** (1988) 2931.
22. S. P. BUGAEV, K. V. OSKOMOV and N. S. SOCHUGOV *Surf. Coat. Technol.* **156** (2002) 311.
23. L. YU, *Ostrovskaya. Vacuum* **18** (2003) 219.
24. FUJIHANA, TAKANOBU, SEKIQUCHI, *et al., Surf. Coat. Technol.* **51** (1992) 19.

Received 22 November 2004
and accepted 8 April 2005